ISSN 1075-7015, Geology of Ore Deposits, 2015, Vol. 57, No. 3, pp. 213–225. © Pleiades Publishing, Ltd., 2015.
Original Russian Text © L.I. Marushchenko, I.A. Baksheev, E.V. Nagornaya, A.F. Chitalin, Yu.N. Nikolaev, I.A. Kal'ko, V.Yu. Prokofiev, 2015, published in Geologiya Rudnykh Mestorozhdenii, 2015, Vol. 57, No. 3, pp. 239–252.

# Quartz–Sericite and Argillic Alterations at the Peschanka Cu–Mo–Au Deposit, Chukchi Peninsula, Russia

**L. I. Marushchenko[a], I. A. Baksheev[a], E. V. Nagornaya[b], A. F. Chitalin[c], Yu. N. Nikolaev[a], I. A. Kal'ko[a], and V. Yu. Prokofiev[d]**

[a] *Mocow State University, Moscow, 119234 Russia*

[b] *Vernadsky State Geological Museum, Russian Academy of Sciences, ul. Mokhovaya 11, str. 11, Moscow, 125009 Russia*

[c] *Regional Mining Company LLC, ul. Sadovnicheskaya 4, Moscow, 115035 Russia*

[d] *Institute of Geology of Ore Deposits, Petrography, Mineralogy, and Geochemistry, Russian Academy of Sciences, Staromonetny per. 35, Moscow, 119017 Russia*

Received July 22, 2014

**Abstract**—The porphyry Peschanka copper–molybdenum–gold deposit and the Nakhodka ore field located in the Baimka ore trend on the western Chukchi Peninsula are spatially related to monzonitic rocks of the Early Cretaceous Egdykgych Complex. Two types of quartz–sericite metasomatic rocks (QSR) have been identified at both the deposits and the ore field: (I) chlorite–quartz–muscovite rock with bornite and chalcopyrite (porphyry type) and (II) tourmaline–quartz–carbonate–muscovite ± phengite rock accompanied by veins with base-metal mineralization (subepithermal or transitional type), as well as carbonate–quartz–illite rock (argillic alteration) accompanied by veins with precious metal mineralization (epithermal type). The QSR I chlorite evolves from chamosite to clinochlore, which is caused by increasing $H_2S$ activity in mineralizing fluid and precipitation of sulfide minerals. The QSR I clinochlore is significantly depleted in silica as compared with that from the rocks affected by argillic alteration. The chemical composition of muscovite from both quartz–sericite alterations is similar. The QSR II carbonates evolve from calcite through dolomite to siderite, which results from the increasing activity of $CO_2$ followed by the decreasing activity of $H_2S$ in mineralizing fluid. The Mn content in dolomite is similar to that in beresite (quartz–muscovite–carbonate–pyrite metasomatic rock) of the intrusion-related gold deposits. Illite from argillic alteration is depleted in Al as compared with that of postvolcanic epithermal Au–Ag deposits. However, carbonates from the discussed argillic alteration rhodochrosite and Mn-rich dolomite are similar to those from quartz–illite rock at postvolcanic epithermal Au–Ag deposits.

**DOI:** 10.1134/S1075701515030034

## INTRODUCTION

Porphyry deposits are the main source of copper all over the world. In Russia, these deposits are located in the Ural, Kuznetsk Alatau, Eastern Syan, Chukotka, Sikhote-Alin, and Kamchatka folded areas. The largest deposits in Russia are Aksug in Tuva and Peschanka in the Chukchi Peninsula; the latter, along with the Nakhodka ore field (NOF), is situated in the Baimka Cu–Mo–Au trend located 200 km south of Bilibino. This trend comprises four porphyry copper fields (from north to south): Yuryakh (YOF), Peschanka (total copper reserves about 6 Mt) Nakhodka (copper reserves about 3 Mt) (Chitalin et al., 2013), and Omchak, which were discovered in the late 1960 to early 1970s and were explored up to early 1990s (Migachev, 1984; Migachev et al., 1995; Kaminskii, 1989; Shapovalov, 1990; Volchkov, 1982). Prospecting and exploration were renewed in 2009 and further researches in this region were feasible.

Corresponding author: L.I. Marushchenko. E-mail: luba.rogacheva@gmail.com

Several types of alteration are conventionally identified at porphyry copper deposits: biotite–potassium feldspar–quartz (potassic), propylitic, quartz–sericite, and argillic. The first type of alteration forms an internal zone of metasomatic aureole with negligible Cu–Mo mineralization. The outer zone is barren propylitic. The quartz–sericite alteration are located within the potassic zone and localized above it, accompanying the porphyry mineralization. Epithermal precious-metal mineralization is spatially related to argillic alteration. In addition, the carbonate–base-metal mineralization frequently developed at porphyry molybdenum–copper deposits (Corbett and Leach, 1998) is regarded as transitional from porphyry to the epithermal stage. Sillitoe (2010) has proposed calling it subepithermal. At most porphyry copper deposits related to granodiorite, this type of mineralization is spatially related to propylitic alteration. The Mount Milligan deposit in Canada related to monzonitic rocks exemplifies subepithermal veins and veinlets accompanied by wall-rock alteration composed of quartz, chlorite, sericite, tourmaline, and carbonates

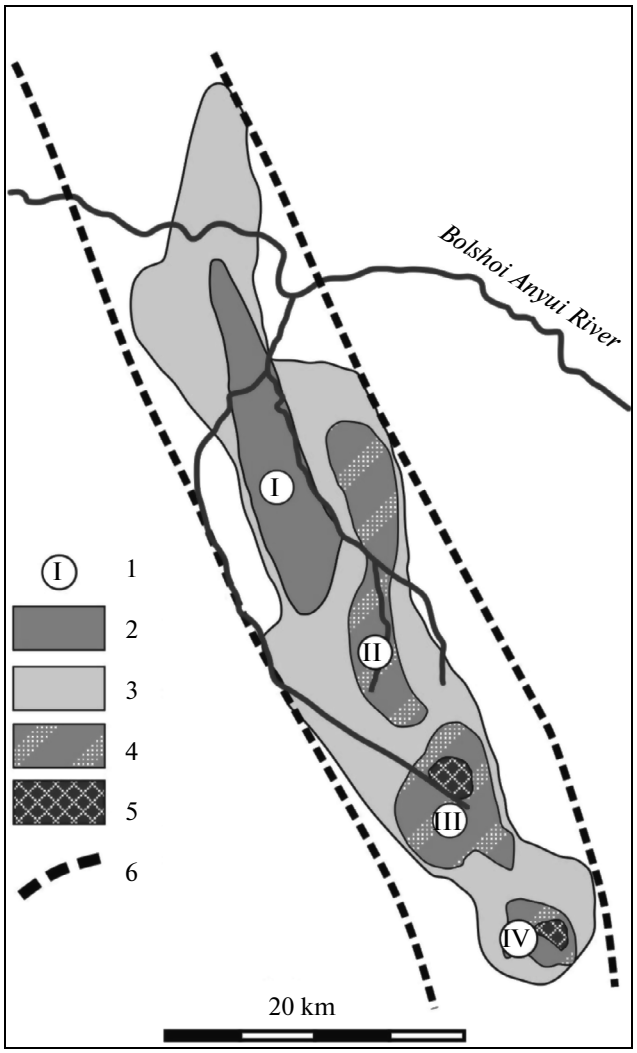


**Fig. 1.** Location of ore fields within the Baimka trend. (1) Ore field, (2–5) Types of hydrothermal alteration: (2) potassic, (3) propylitic, (4) quartz–sericite zones cutting potassic alteration, (5) argillic. (I) Yuryakh, (II) Peschanka, (III) Nakhodka, (IV) Omchak.

(Le Fort et al., 2011). Similar metasomatic rock accompanied by veins with galena, sphalerite, and chalcopyrite was found at the Peschanka deposit and NOF, but within intrusions. At the Vesenny deposit in NOF, quartz–carbonate veins with precious metal mineralization are hosted in quartz–illite alteration containing Mn-rich carbonates.

The objective of this study is to specify the mineralogical features of quartz–sericite alteration related to porphyry and subepithermal mineralization and to show a difference in argillic alteration at porphyry and postvolcanic epithermal Au–Ag deposits.

## BRIEF GEOLOGY, ALTERATIONS AND ORES

The Baimka trend is a part of the Oloi metallogenic zone, where Cu–Mo–Au porphyry systems were formed in a continental arc environment. Porphyry deposits are related to the Early Cretaceous Egdykgich Complex, whose monzonitic bodies intrude into the Upper Jurassic volcanic and volcanic–sedimentary sequence (Fig. 1). Nikolaev et al. (in press) have reported in detail the geology of the Baimka trend and separate ore fields and deposits.

Four types of altered rocks were identified at the deposits and prospects within the Baimka trend: (1) biotite–potassium feldspar–quartz (BPFQR), (2) propylite, (3) quartz–sericite (QSR), and (4) argillic.

Biotite–potassium feldspar–quartz metasomatic rock forming internal zone of metasomatic aureole is predominant at the Peschanka deposit and prospects of YOF. Propylite occurring at all locations of the Baimka trend forms an outer zone of hydrothermal alteration replacing intrusive, volcanic, and volcanic–sedimentary rocks. The abundance of quartz–sericite alteration increases from the YOF to NOF, indicating the decreasing erosion level of ore fields. Quartz–sericite alteration is sporadic in YOF. At the Peschanka deposit, it forms zones cutting BPFQR, while in NOF it is the most abundant. Carbonate–quartz–ilite metasomatic rock to which epithermal precious metal mineralization of the Vesenny deposit is related is abundant in NOF. Metasomatic rock containing illite is attributed to argillic alteration (Zharikov et al., 1998). Altered rock with illite was found neither at the Peschanka deposit nor in the YOF. In the Omchak ore field, argillic alteration is represented by calcite–adularia–chlorite rock.

The porphyry Cu–Mo mineralization spatially related to potassic and quartz–sericite zones comprises impregnation and stockworks of quartz veins and veinlets with bornite, chalcopyrite, molybdenite, pyrite, and Ti-free magnetite. The average Cu and Mo grades at Peshanka and Nakhodka are 0.53% and 140 g/t and 0.34% and 54 g/t, respectively (Chitalin et al., 2013).

The Re/Os model age of molybdenite from the Peschanka deposit and NOF is 142.6 ± 6.9 and 143.3 ± 3.0 Ma, respectively (Baksheev et al., 2014), which is proximate, within error, to the U/Pb age of the Egdykgych Complex 139.5 ± 0.5 – 140.3 ± 0.5 Ma (Kotova et al., 2012). The minerals of the carbonate–base-metal assemblage fill veins and veinlets hosted in both potassic and quartz–sericite alterations. Galena and sphalerite are the major ore minerals; chalcopyrite and tennantite–tetrahedrite are minor; enargite, Te minerals (hessite, native tellurium), and native gold are occasional. Economic epithermal mineralization spatially related to carbonate–quartz–illite altered rock was found at the Vesenny deposit in the southern NOF, with average grade as follows: 2.9 g/t Au, 56 g/t Ag, 0.9% Pb + Zn, and 0.15% Cu. The ore consists of As-rich pyrite (up to 10 wt % As), sphalerite, galena, chalcopyrite, Zn-rich tennantite to Ag-bearing (4 wt % Ag) Zn-rich tetrahedrite, low-fineness native gold, elec-

trum, and hessite; petzite, stützite, pearceite, and acanthite are rare. Low fineness gold (756–857) and electrum (657–743) enclosing and filling fractures in pyrite, galena, and tennantite–tetrahedrite are intimately intergrown with hessite and petzite.

In the Omchak ore field, epithermal Ag mineralization, represented by naumannite, Se-rich pearceite (up to 4 wt % Se), and acanthite, was found along with ordinary porphyry molybdenum–copper mineralization. In addition, rare algodonite was identified (Nikolaev et al., in press).

## ANALYTICAL METHODS

Electron microscopic study of rock-forming minerals and the determination of their chemical composition were performed with a Jeol JSM-6480LV SEM equipped with an INCA-Energy 350 EDS and INCA Wave 500 WDS at the Laboratory of high spatial resolution analytical techniques, Division of Petrology, Moscow State University. Back-scattered electron images were obtained at an accelerating voltage of 20 kV and a current intensity of about 2 nA. The chemical composition of minerals was measured with EDS at an accelerating voltage of 20 kV and current intensity of 2 ± 0.05 nA. The content of F in tourmaline and micas was measured with WDS (TAP crystal) at an accelerating voltage of 20 kV and current intensity of about 23 nA using $MgF_2$ as reference material. Stoichiometric oxides and silicates with measured compositions were used as standards for other elements. We used XPP-software for the correction procedures (INCA, version 15a, Oxford Instrument). The uncertainty of single measurement does not exceed 1.5% relative.

Tourmaline formulae were normalized on the basis of 15 cations, excluding Na, Ca, and K, i.e., assuming no vacancies at the tetrahedral or octahedral sites, and an insignificant content of Li (Henry et al., 2011). Charge-balance constraints were used to estimate the amounts of $OH^-$ and $O^{2-}$ associated with the *V* and *W* anion sites in the structural formula. The proportion of X-site vacancies ( ) was calculated using stoichiometric constraints by means of 1 – (Na + Ca + K). The amount of $B_2O_3$ was calculated from stoichiometric constraints. $Fe^{2+}/Fe^{3+}$ ratio was calculated from charge-balance constraints. The formulae of chlorite and sericite were normalized on the basis of 10 cations and 22 anions, respectively. The $H_2O$ content in these minerals was calculated from stoichiometric constraints. The crystal chemical formulae of the dolomite and calcite group minerals were calculated on the basis of 2 and 1 metal atoms, respectively. Average contents as atoms per formula unit (apfu) or wt % in the discussed minerals are given below.

## RESULTS

Quartz–sericite altered rocks are light gray, whitish with lepidogranoblastic and relict porphyritic textures; their structure is massive. Muscovite, phengite, and quartz are the major rock-forming minerals; chlorite, albite, tourmaline and carbonates are minor constituents. Rock-forming minerals of replaced magmatic or metasomatic rocks remained at weak hydrothermal alteration: potassium feldspar, plagioclase, biotite, and magnetite. Rutile and apatite are accessory minerals of quartz–sericite metasomatic rocks. Quartz–sericite rocks are divided into two types in mineralogy: (I) chlorite–quartz–muscovite rock (QSR I) with bornite and chalcopyrite (porphyry type) and (II) tourmaline–quartz-carbonate–muscovite ± phengite rock (QSR II) accompanying veins with base-metal mineralization (subepithermal or transitional type). Carbonate–quartz–illite argillic rock is light gray, fine-grained, and massive. This rock is composed of illite, Mn-rich dolomite, rhodochrosite, quartz, rare chlorite, and relict albite and sericite.

Vertical zoning at the Nakhodka and Pryamoi prospects in NOF is remarked: metasomatic rocks with illite at the upper level grade to QSR I and QSR II at a depth of 100–200 m. At the Vesenny deposit in NOF, carbonate–quartz-illite argillic alteration develops down to 300 m below the surface. Argillic alteration is found also at the flanks of the Vesenny III prospect in NOF.

*Chlorites* of chlorite–quartz–muscovite rock studied here are fine split flakes up to 40 μm in size and coarse-lamellar aggregates up to 300 μm in size. Chlorites replace magmatic biotite, amphiboles, pyroxenes, and phlogopite of BPFQR.

Electron microscopy revealed zoning in chlorite grains. A back-scattered electron image (Fig. 2a) shows that the darker rims of chlorite lamellae depleted in Fe are close to sulfide minerals, whereas the lighter cores are enriched in Fe; chlorites enriched in Fe occur also in barren altered rocks. It is probable that chlorite enriched in Fe predates that depleted in Fe; the latter crystallized when sulfide minerals precipitated.

According to the classification of Bailey (1980), the chlorites studied here are categorized as chamosite and clinochlore (Table 1, Fig. 3). In general, chlorites of the Peschanka deposit are depleted in silica as compared with those of NOF. The clinochlore and chamosite of the Peschanka deposit are enriched in Mn (0.19 and 0.12 apfu, respectively) as compared with those from NOF (0.06 and 0.03 apfu, respectively). The concentration of other trace elements in chlorite does not exceed a few hundredths apfu.

Chlorite from argillic rocks of NOF is fine (up to 10 μm) flakes of clinochlore having a higher Si content (3.58 apfu) than that of QSR I (2.87–3.03 apfu Si); Mn content does not exceed a few hundredths apfu.

*White micas* are muscovite, phengite, and illite. Muscovite and illite are fine-flake split aggregates of

**Table 1.** Chemical composition (wt %) of the chlorite group minerals from quartz–sericite altered rocks at the Peschanka deposit and in the Nakhodka ore field

| Component | 1 | | 2 | | 3 |
|---|---|---|---|---|---|
| | clinochlore ($n = 22$) | chamosite ($n = 6$) | clinochlore ($n = 39$) | chamosite ($n = 5$) | clinochlore ($n = 6$) |
| $SiO_2$ | 27.82 | 26.91 | 29.50 | 26.64 | 34.59 |
| $TiO_2$ | 0.02 | 0.13 | 0.06 | 0.08 | 0.03 |
| $Al_2O_3$ | 19.95 | 20.93 | 18.67 | 19.60 | 15.49 |
| FeO | 20.19 | 28.03 | 17.87 | 28.11 | 15.21 |
| MnO | 2.10 | 1.33 | 0.69 | 0.33 | 0.18 |
| MgO | 17.69 | 10.59 | 20.26 | 12.99 | 20.74 |
| CaO | 0.13 | 0.11 | 0.13 | 0.06 | 0.66 |
| $Na_2O$ | 0.24 | 0.26 | 0.22 | 0.13 | 0.24 |
| $H_2O$ | 11.34 | 10.71 | 11.36 | 10.95 | 11.95 |
| F | b.d.l. | b.d.l. | 0.02 | 0.07 | b.d.l. |
| 2F=O | | | 0.01 | 0.03 | |
| Total | 99.48 | 99.00 | 98.77 | 98.93 | 99.09 |
| Coefficients in crystal chemical formulae | | | | | |
| Si | 2.887 | 2.931 | 3.033 | 2.866 | 3.580 |
| $Al^T$ | 1.113 | 1.069 | 0.967 | 1.134 | 0.420 |
| Total *T* | 4.000 | 4.000 | 4.000 | 4.000 | 4.000 |
| $Al^A$ | 1.326 | 1.627 | 1.294 | 1.351 | 1.468 |
| Fe | 1.752 | 2.563 | 1.537 | 2.529 | 1.316 |
| Mg | 2.736 | 1.677 | 3.104 | 2.083 | 3.198 |
| Ti | 0.001 | 0.010 | 0.005 | 0.007 | 0.002 |
| Mn | 0.185 | 0.123 | 0.060 | 0.030 | 0.016 |
| Ca | 0.015 | 0.013 | 0.014 | 0.007 | 0.073 |
| Na | 0.047 | 0.055 | 0.044 | 0.028 | 0.049 |
| Total *A* | 6.062 | 6.068 | 6.058 | 6.035 | 6.122 |
| F | | | 0.007 | 0.024 | 0.000 |
| $OH^-$ | 7.854 | 7.670 | 7.796 | 7.864 | 7.353 |
| $O^{2-}$ | 0.146 | 0.330 | 0.204 | 0.136 | 0.324 |
| $Fe_{tot}/(Fe_{tot}+ Mg)$ | 0.39 | 0.62 | 0.33 | 0.55 | 0.29 |

(1) QSR I of the Peschanka deposit, (2, 3) Nakhodka ore field: (2) QSR I, (3) QSR II. Here and after, b.d.l. denotes that the content of element is below detection and *n* is number of analyses.

20–30 μm in size and euhedral lamellae up to 100 μm in size. In chlorite–quartz–muscovite rock, muscovite and phengite are intimately intergrown with albite or replace earlier chlorite and potassium feldspar (Fig. 2c). Mica from QSR II is intergrown with dolomite and tourmaline (Fig. 2d). Illite from argillic alteration occurs as fine flakes up to a few tens of microns and aggregates of these flakes.

The chemical composition of muscovite from both types of quartz–sericite alteration of the Peschanka deposit and NOF is identical (Table 2). The mineral contains few Na up to 0.07 apfu and Ti up to 0.02 apfu; the $Fe_{tot}/(Fe_{tot} + Mg)$ value ranges from 0.38 to 0.41. Phengite of both types of quartz–sericite rocks at the Peschanka deposit is richer in Fe ($Fe_{tot}/(Fe_{tot} + Mg) = 0.50$), Na (0.04 apfu) and Ti (up to 0.02 apfu), than that in NOF (0.21, 0.01 apfu, and 0.01 apfu, respectively).

Argillic illite is richer in Si (up to 3.31 apfu) than muscovite and phengite. The K content in the mineral decreases toward the flake rims from 9.17 to 8.03 wt % $K_2O$. The concentration of trace Na, Ti, and Ca does not exceed a few hundredths apfu.

*Tourmaline* at the Peschanka deposit and NOF found from the second type of quartz–sericite rock is associated with base-metal sulfides. The mineral is locally common and occurs as both light green irregular-shaped isolated grains up to 50 μm in size (Fig. 2b) and radial aggregates up to 300 μm in diameter (Fig. 2d).

Electron microscopy revealed three generations of tourmaline from radial aggregates at the Peschanka deposit. Tourmaline of the first generation occurs as inhomogeneous crystals resulting from a variable content of Fe and Al. Average contents of Fe, Al, and Mg are 1.56, 5.77, and 1.60 apfu, respectively; the average X-site vacancy proportion is 0.11 apfu (Table 3). The second generation of tourmaline overgrows tourmaline I (Fig. 2d) and forms proper grains. Cores of the tourmaline II grains are depleted in Fe (a few wt %) as compared with the rims (up to 11 wt %). Average Fe content in tourmaline II 0.85 apfu is slightly lower

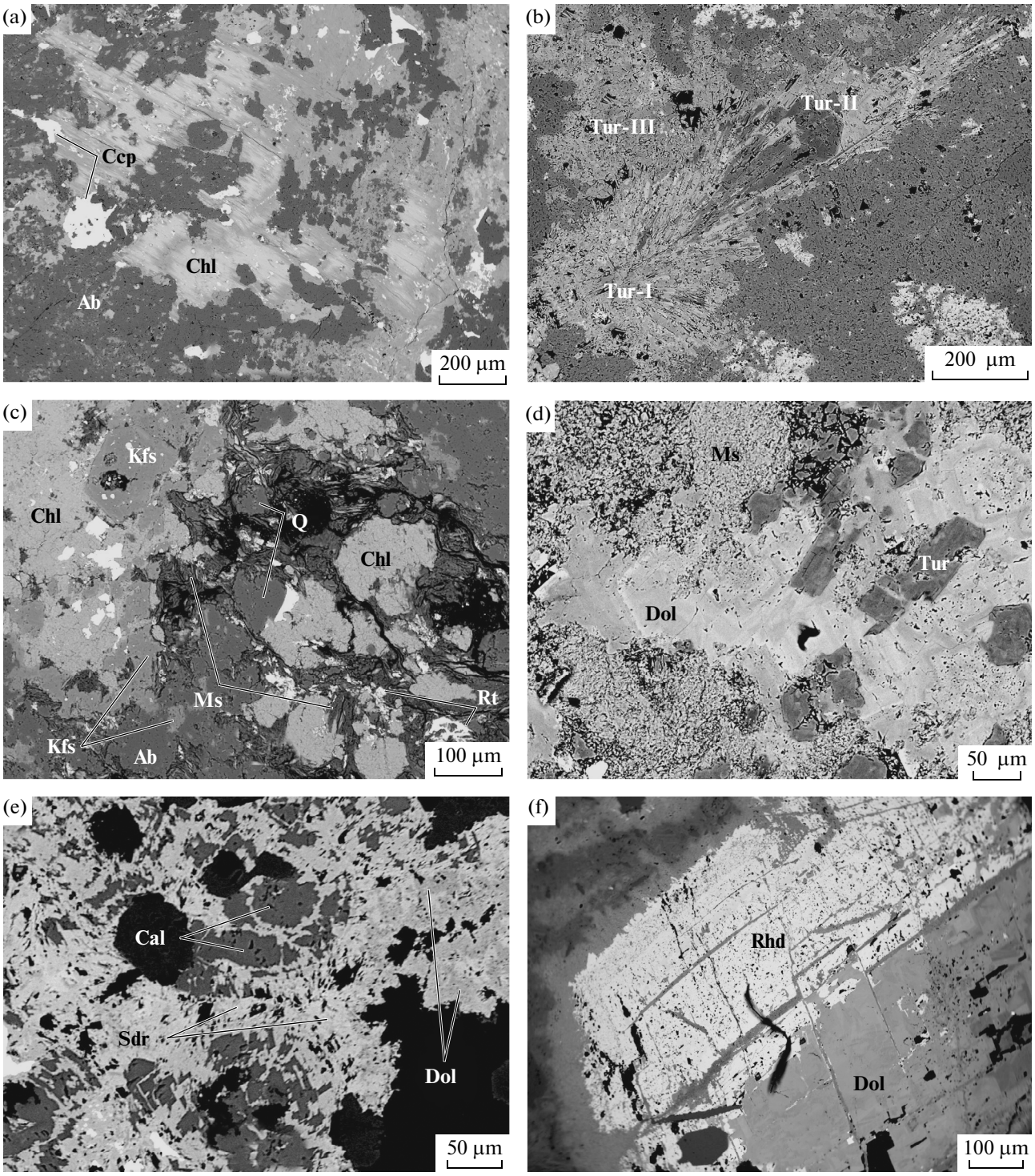


**Fig. 2.** Back-scattered electron images of minerals from altered rocks of the Peschanka deposit and Nakhodka ore field. (a) Zoned chlorite flakes intergrown with chalcopyrite in quartz–albite matrix, (b) first, second and third tourmaline generations, (c) oscillatory zoned dolomite crystals associated with weakly zoned tourmaline in muscovite aggregates, (c) muscovite replacing chlorite and potassic feldspar in quartz–albite matrix (d) dolomite overgrew calcite and is replaced by siderite, (e) rhodochrosite overgrew Mn-rich dolomite. (Ab) Abite, (Cal) calcite, (Ccp) chalcopyrite, (Chl) chlorite, (Dol) dolomite, (Kfs) potassium feldspar, (Ms) muscovite, (Q) quartz, (Rhd) rhodochrosite, (Rt) rutile, (Sdr) siderite, (Tur) tourmaline.

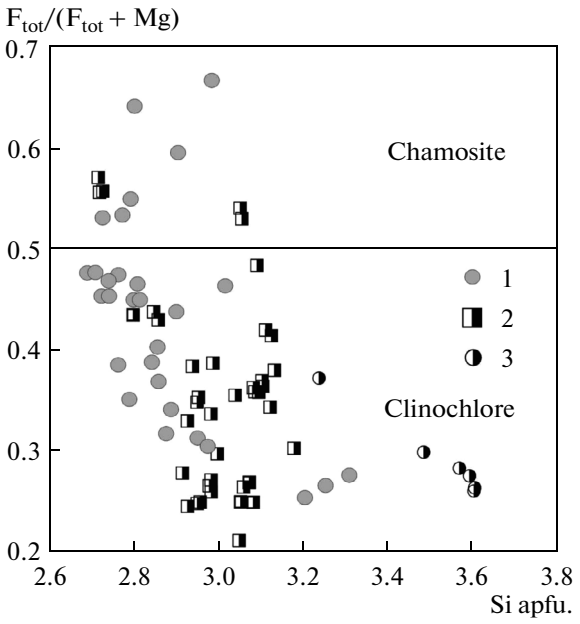


**Fig. 3** Classification diagram (Bailey, 1980) of chlorites from altered rocks of the Peschanka deposit and Nakhodka ore field. (1) Peschanka deposit, QSR I, (2, 3) Nakhodka ore field: (2) QSR I, (3) argillic rock.

than that in tourmaline I. The Al and Mg concentrations are 6.28 and 1.95 apfu, respectively; X-site vacancy proportion is 0.15 apfu. Tourmaline of the third generation contains 6.3 apfu Al and 1.10 apfu Fe; the average Mg concentration is 1.76 apfu; the average X-site vacancy proportion is 0.18 apfu. Ti and Ca content does not exceed a few tenths apfu through the three generations.

Two generations of tourmaline are found in NOF. Tourmaline of the first generation occurs as large aggregates composed of fine misoriented weakly zoned crystals. Average Fe, Mg, and Al contents are 1.11, 1.76, and 6.91 apfu, respectively; the average X-site vacancy proportion is 0.16 apfu. The second generation of tourmaline occurs as overgrowth rims on tourmaline I and isolated unzoned crystals up to a few ten microns in length. The contents of Fe (0.77 apfu), Mg (1.64 apfu), and Al (6.59 apfu) is lower in tourmaline II than those in tourmaline I. X-site vacancy proportion is 0.16 apfu. As with tourmaline from the Peschanka deposit, the Ca and Ti content in the NOF tourmaline is a few tenths of apfu.

The compositions of tourmalines from quartz–sericite altered rocks of the Peschanka deposit and NOF are below the schorl–dravite join and parallel to the $AlO(FeOH)_{-1}$ exchange vector (Fig. 4a).

The tourmalines studied here are classified as dravite and oxy-dravite according to Henry et al. (2011).

*Carbonates* were identified in QSR II and argillic alteration. The QSR II carbonates, calcite, siderite, magnesite, and dolomite (Table 4), occur as isolated crystals and aggregates of crystals, pockets, and veinlets. The isolated crystals reach a few hundred microns in size. Microscopic observation revealed that the earliest calcite is overgrown by later dolomite and/or magnesite. Siderite replacing dolomite and magnesite is the latest (Fig. 2e).

Carbonates of argillic alteration are calcite, dolomite, and rhodochrosite. These minerals together with quartz, sphalerite, galena, fahlores, hessite, and native gold fill veinlets and pockets. The earliest calcite is followed by rhodochrosite overgrown by Mn-rich dolomite.

*Calcite* from tourmaline–quartz–carbonate–muscovite ± phengite rock overgrowing feldspar occurs as isolated crystals and aggregates of the crystals in argillic alteration. The QSR II calcite at the Peschanka deposit is richer in Fe (Fe/(Fe +Mg) = 0.77) than that in NOF (0.33). In the both cases, Mn content does not exceed a few hundredths apfu. The $Fe_{tot}/(Fe_{tot} + Mg)$ value and Mn content in calcite from the rocks affected by argillic alteration is 0.43 and 0.4 apfu, respectively.

*The dolomite of QSR II* intimately intergrown with sericite, quartz, and tourmaline is irregular-shaped zoned crystals. The zoning is caused by the variable Fe content. The QSR II dolomite at the Peschanka deposit and NOF is characterized by a close Fe/(Fe + Mg) value (0.29 and 0.20, respectively) and low Mn content, up to a few hundredths of apfu.

Dolomite from argillic alteration overgrows and replaces rhodochrosite (Fig. 2f) and fill pockets and veinlets in metasomatic rock. In contrast to dolomite from QSR II, the zoning of dolomite crystals is caused by alternation of zones enriched and depleted in Mn. Average Fe and Mn content in dolomite is 0.18 and 0.15 apfu, respectively.

*Magnesite* established only in QSR II of NOF occurs as irregular-shaped grains. It appeared to crystallize close to dolomite. The Mn and Ca content in the mineral is 0.01 apfu.

*Siderite* was found in QSR II at both Peschanka and NOF. It overgrows earlier carbonates: dolomite at Peshanka, and dolomite and magnesite in NOF. The mineral is enriched in Mg (up to 0.3 apfu); the Ca and Mn contents are negligible.

*Rhodochrosite* was identified in argillic alteration of NOF. It occurs as euhedral crystals up to a few mm in size, which are replaced by Mn-rich dolomite. The mineral has insignificant Mn and Ca admixture, up to 0.03 apfu.

## DISCUSSION

The rock-forming constituents of quartz–sericite rocks at the Peschanka deposit and NOF (micas, chlorite, tourmaline, and carbonates) contain a significant amount of Mg, which is caused by the replacement of rocks with minerals enriched in Mg. In the case of

**Table 2.** Average chemical composition (wt %) of white micas from altered rocks of the Peschanka deposit and Nakhodka ore field

| Component | 1 | | 2 | | 3 | | 4 | 5 |
|---|---|---|---|---|---|---|---|---|
| | muscovite ($n = 16$) | phengite ($n = 2$) | muscovite ($n = 17$) | phengite ($n = 7$) | muscovite ($n = 10$) | phengite | muscovite ($n = 12$) | illite ($n = 47$) |
| $SiO_2$ | 47.05 | 48.95 | 46.67 | 49.31 | 47.36 | 49.97 | 45.67 | 50.25 |
| $TiO_2$ | 0.32 | 0.26 | 0.28 | 0.30 | 0.24 | 0.07 | 0.35 | 0.11 |
| $V_2O_3$ | b.d.l. | b.d.l. | b.d.l. | b.d.l. | 0.13 | 0.16 | 0.04 | 0.11 |
| $Al_2O_3$ | 32.96 | 29.04 | 32.39 | 30.63 | 32.63 | 31.27 | 34.57 | 31.49 |
| $FeO_{tot}$ | 2.14 | 3.91 | 2.87 | 2.62 | 2.28 | 1.06 | 1.97 | 1.54 |
| MnO | b.d.l. | b.d.l. | 0.04 | 0.07 | b.d.l. | 0.03 | 0.02 | 0.04 |
| MgO | 1.98 | 2.18 | 2.10 | 2.00 | 1.94 | 2.30 | 1.59 | 2.18 |
| CaO | 0.01 | 0.05 | 0.03 | 0.04 | 0.07 | 0.22 | 0.05 | 0.19 |
| $K_2O$ | 10.12 | 10.53 | 10.44 | 10.29 | 10.14 | 9.83 | 10.05 | 9.07 |
| $Na_2O$ | 0.45 | 0.29 | 0.37 | 0.15 | 0.30 | 0.07 | 0.52 | 0.13 |
| $H_2O$ | 4.48 | 4.44 | 4.46 | 4.5 | 4.43 | 4.53 | 4.36 | 4.54 |
| F | b.d.l. | b.d.l. | b.d.l. | b.d.l. | 0.11 | b.d.l. | 0.22 | 0.14 |
| 2F=O | | | | | 0.05 | | 0.06 | 0.05 |
| Total | 99.52 | 99.64 | 99.64 | 99.91 | 99.69 | 99.51 | 99.46 | 99.82 |
| Coefficients in crystal chemical formulae | | | | | | | | |
| Si | 3.146 | 3.300 | 3.138 | 3.283 | 3.166 | 3.303 | 3.063 | 3.307 |
| $Al^T$ | 0.854 | 0.700 | 0.862 | 0.717 | 0.834 | 0.697 | 0.937 | 0.693 |
| Total *T* | 4.000 | 4.000 | 4.000 | 4.000 | 4.000 | 4.000 | 4.000 | 4.000 |
| $Al^M$ | 1.744 | 1.606 | 1.703 | 1.687 | 1.736 | 1.738 | 1.796 | 1.750 |
| Mg | 0.197 | 0.219 | 0.210 | 0.199 | 0.194 | 0.226 | 0.158 | 0.213 |
| $Fe_{tot}$ | 0.120 | 0.220 | 0.161 | 0.146 | 0.127 | 0.059 | 0.111 | 0.085 |
| Mn | | | 0.002 | 0.004 | | 0.002 | 0.001 | 0.002 |
| Ti | 0.016 | 0.013 | 0.014 | 0.015 | 0.012 | 0.003 | 0.017 | 0.005 |
| V | | | | | 0.007 | 0.008 | 0.002 | 0.006 |
| Total *M* | 2.077 | 2.058 | 2.090 | 2.051 | 2.076 | 2.036 | 2.085 | 2.061 |
| Ca | 0.001 | 0.003 | 0.002 | 0.003 | 0.005 | 0.016 | 0.003 | 0.013 |
| Na | 0.058 | 0.038 | 0.049 | 0.020 | 0.039 | 0.010 | 0.068 | 0.017 |
| K | 0.863 | 0.905 | 0.895 | 0.874 | 0.865 | 0.829 | 0.860 | 0.761 |
| Total *I* | 0.922 | 0.946 | 0.946 | 0.897 | 0.909 | 0.855 | 0.931 | 0.791 |
| $OH^-$ | 2.000 | 2.000 | 2.000 | 2.000 | 1.976 | 2.000 | 1.953 | 1.994 |
| F | | | | | 0.024 | | 0.047 | 0.006 |
| Total *A* | 2.000 | 2.000 | 2.000 | 2.000 | 2.000 | 2.000 | 2.000 | 2.000 |
| $Al_{tot}$ | 2.597 | 2.307 | 2.566 | 2.404 | 2.570 | 2.436 | 2.733 | 2.443 |
| $Fe_{tot}/(Fe_{tot} + Mg)$ | 0.38 | 0.50 | 0.43 | 0.42 | 0.40 | 0.21 | 0.41 | 0.29 |

(1, 2) Peschanka deposit: (1) QSR I, (2) QSR II; (3–5) Nakhodka ore field: (3) QSR I, (4) QSR II, (5) argillic alteration.

**Table 3.** Average chemical composition (wt %) of the tourmaline group minerals from the second type of quartz--sericite altered rock of the Peschanka deposit and in the Nakhodka ore field

| Component | 1 | | | 2 | |
|---|---|---|---|---|---|
| | tourmaline-I ($n = 5$) | tourmaline-II ($n = 14$) | tourmaline-III ($n = 18$) | tourmaline-I ($n = 12$) | tourmaline-II ($n = 7$) |
| $B_2O_3$ | 10.32 | 10.50 | 10.76 | 10.59 | 10.61 |
| $SiO_2$ | 35.10 | 35.21 | 35.71 | 35.88 | 36.27 |
| $TiO_2$ | 0.97 | 0.82 | 0.26 | 0.30 | 0.40 |
| $Al_2O_3$ | 28.98 | 32.30 | 32.38 | 32.10 | 34.13 |
| FeO | 11.07 | 6.21 | 7.26 | 7.91 | 5.62 |
| MgO | 6.37 | 7.91 | 7.16 | 7.14 | 6.73 |
| CaO | 0.77 | 0.62 | 0.45 | 0.10 | 0.19 |
| $K_2O$ | 0.03 | 0.03 | b.d.l. | 0.02 | 0.39 |
| $Na_2O$ | 2.27 | 2.30 | 2.31 | 2.61 | 2.50 |
| $H_2O$ | 3.53 | 3.50 | 3.46 | 3.56 | 3.26 |
| F | b.d.l. | b.d.l. | 0.04 | b.d.l. | b.d.l. |
| 2F=O | | | 0.02 | | |
| Total | 99.42 | 99.39 | 99.80 | 100.21 | 100.08 |
| Coefficients in crystal chemical formulae | | | | | |
| B | 3.000 | 3.000 | 3.000 | 3.000 | 3.000 |
| Si | 5.934 | 5.812 | 5.899 | 5.903 | 5.944 |
| $^{T}$Al | 0.066 | 0.188 | 0.101 | 0.097 | 0.056 |
| Total *T* | 6.000 | 6.000 | 6.000 | 6.000 | 6.000 |
| $^{Z}$Al | 5.708 | 6.000 | 6.000 | 6.000 | 6.000 |
| $^{Z}Fe^{3+}$ | 0.081 | | | | |
| $^{Z}$Mg | 0.211 | | | | |
| Total *Z* | 6.000 | 6.000 | 6.000 | 6.000 | 6.000 |
| $Al^{Y}$ | 0.000 | 0.096 | 0.202 | 0.125 | 0.536 |
| Mg | 1.393 | 1.945 | 1.762 | 1.750 | 1.645 |
| $Fe^{2+}$ | 1.483 | 0.857 | 1.003 | 1.063 | 0.771 |
| $^{Y}Fe^{3+}$ | | | | 0.025 | |
| Ti | 0.123 | 0.102 | 0.032 | 0.037 | 0.049 |
| Total *Y* | 2.999 | 3.000 | 2.999 | 3.000 | 3.001 |
| Na | 0.745 | 0.735 | 0.741 | 0.834 | 0.793 |
| $^{X}$ | 0.108 | 0.149 | 0.181 | 0.144 | 0.093 |
| Ca | 0.140 | 0.109 | 0.079 | 0.017 | 0.033 |
| K | 0.007 | 0.007 | | 0.005 | 0.081 |
| Total *X* | 1.000 | 1.000 | 1.000 | 1.000 | 1.000 |
| $OH^{V}$ | 3.000 | 3.000 | 3.000 | 3.000 | 3.000 |
| $OH^{W}$ | 1.000 | 0.930 | 0.916 | 1.000 | 0.482 |
| $O^{W}$ | 0.000 | 0.070 | 0.063 | 0.000 | 0.518 |
| F | | | 0.021 | | |
| Total *W* | 1.000 | 1.000 | 1.000 | 1.000 | 1.000 |
| $Fe_{tot}/(Fe_{tot} + Mg)$ | 0.49 | 0.31 | 0.36 | 0.38 | 0.32 |
| $^{X}/(^{X} + Na)$ | 0.13 | 0.17 | 0.20 | 0.15 | 0.10 |
| $Al_{tot}$ | 5.774 | 6.284 | 6.304 | 6.223 | 6.083 |
| $Fe_{tot}$ | 1.565 | 0.857 | 1.003 | 1.088 | 0.771 |

(1) Peschanka deposit, (2) Nakhodka ore field. $^{X}$ denotes *X*-site vacancy.

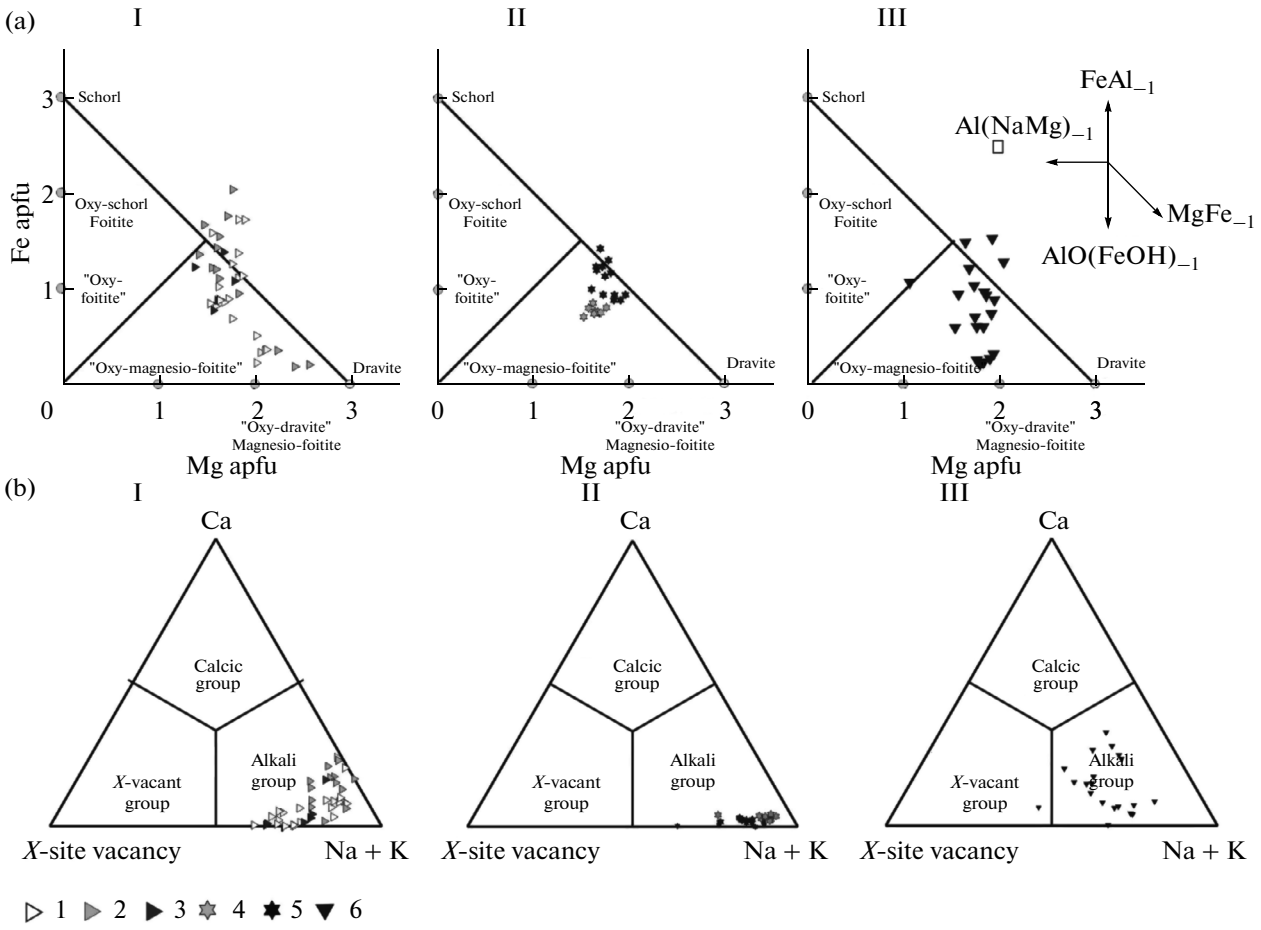


**Fig. 4.** Variations in the composition of tourmaline supergroup minerals from quartz–sericite rocks of (I) the Peschanka deposit, (II) Nakhodka ore field, and (III) Olkhovka deposit, Chukchi Peninsula. (a) Fe versus Mg diagram, (b) X-site vacancy–Ca–(Na+K) classification diagram (Henry et al., 2011). (1–3) Peschanka deposit: (1) generation I, (2) generation II, (3) generation III; (4, 5) Nakhodka ore field: (4) generation I, (5) generation II; (6) Olkhovka deposit, Chukchi Peninsula.

magmatic rocks, these are biotite, diopside, and magnesiohastingsite. In the case of biotite–potasium feldspar–quartz altered rock, this is biotite. Mg-rich minerals of replaced propytlite are chlorite and tremolite–actinolite. The major mineralogical features of altered rocks are given in Table 5.

Clinochlore and chamosite of chlorite–quartz–muscovite rock are similar in chemical composition to those of quartz–sericite rocks reported at the other porphyry copper deposits (Dilles et al., 2012). The compositional evolution of the QSR I chlorites from early chamosite to late clinochlore is caused by the increasing activity of $H_2S$ in mineralizing fluids resulting in the precipitation of sulfide minerals with predominant incorporation of Fe into the latter. Clinochlore of argillic alteration differs from that in QSR I in elevated Si content and lower Al concentration. Clinochlore with a high Si content is typical of argillic alteration of geothermal systems (Martinez-Serrano and Dubois, 1998).

White micas of porphyry copper deposits are reported in many publications (Sotnikov et al., 2002; Alva-Jimenez et al., 2011; Dilles et al., 2012). White micas are rock-forming constituents of metasomatic rocks at intrusion-related and postvolcanic epithermal gold deposits. An Al versus Si diagram was constructed to compare the chemical composition of white micas from various types of altered rocks in the Baimka trend and other types of ore deposits (Fig. 5). The compositions of white micas from QSR I and QSR II fall into the field of porphyry copper quartz–sericite rocks and the field of white micas typical of alteration at plutonogenic gold deposits. Illite from postvolcanic epithermal deposits is richer in Al (Dilles et al., 2012). The compositions of illite from carbonate–quartz–illite altered rock in the Baimka trend fall into the overlap area of these fields and the field of porphyry copper illite. Thus, the composition of illite allows distinguishing argillic alteration related to porphyry and postvolcanic epithermal systems.

At the Peschanka deposit and NOF, tourmaline was found only from QSR II. However, Rogacheva and

**Table 4.** Average chemical composition (wt %) of carbonates from altered rocks of the Peschanka deposit and Nakhodka ore field

| Component | 1 | | | 2 | | | | 3 | | |
|---|---|---|---|---|---|---|---|---|---|---|
| | calcite ($n = 13$) | dolomite ($n = 20$) | siderite ($n = 6$) | calcite ($n = 7$) | dolomite ($n = 40$) | magnesite ($n = 3$) | siderite ($n = 5$) | calcite ($n = 11$) | rhodochrosite | dolomite ($n = 23$) |
| CaO | 52.35 | 29.01 | 1.55 | 55.02 | 28.84 | 0.22 | 1.23 | 51.99 | 1.58 | 29.82 |
| MgO | 0.30 | 13.93 | 6.25 | 0.44 | 16.04 | 25.23 | 11.48 | 0.77 | 1.03 | 12.32 |
| FeO | 0.60 | 9.78 | 48.93 | 0.39 | 6.95 | 27.62 | 45.29 | 1.03 | í.ï.î. | 6.50 |
| MnO | 2.24 | 0.76 | 2.43 | 1.08 | 0.50 | 0.37 | 0.26 | 2.97 | 59.19 | 5.20 |
| Total | 55.49 | 53.48 | 59.16 | 56.93 | 52.33 | 53.44 | 58.26 | 56.76 | 61.80 | 53.84 |
| Coefficients in crystal chemical formulae | | | | | | | | | | |
| Ca | 0.952 | 1.025 | 0.031 | 0.968 | 1.012 | 0.004 | 0.023 | 0.924 | 0.032 | 1.062 |
| Mg | 0.008 | 0.682 | 0.171 | 0.011 | 0.783 | 0.614 | 0.302 | 0.019 | 0.029 | 0.608 |
| Fe | 0.009 | 0.271 | 0.760 | 0.005 | 0.190 | 0.377 | 0.670 | 0.014 | – | 0.181 |
| Mn | 0.032 | 0.021 | 0.039 | 0.015 | 0.014 | 0.005 | 0.004 | 0.043 | 0.939 | 0.147 |
| $Fe_{tot}/(Fe_{tot}+ Mg)$ | 0.76 | 0.28 | 0.81 | 0.33 | 0.2 | 0.38 | 0.69 | 0.43 | – | 0.23 |

(1) Peschanka deposit, QSR I; (2, 3) Nakhodka ore field: (2) QSR II, (3) argillic alteration.

Baksheev (2010) reported that at porphyry copper deposits tourmaline also occurs in carbonate-free quartz–chlorite–muscovite alteration accompanying porphyry mineralization. The triangular diagram (Fig. 4b) shows that tourmaline from carbonate-free quartz–chlorite–muscovite rock is characterized by a much higher Ca content than that from the alteration studied here. A substantial difference in Ca content is caused by the incorporation of this element into carbonates associated with tourmaline at Peschanka and NOF, rather than into silicate mineral. At the same time, chemical substitution $^{Y}Al + {}^{W}O \rightarrow {}^{Y}Fe^{2+} + {}^{W}OH$ remains (Fig. 4a). Thus, the tourmaline from quartz–sericite alteration accompanying subepithermal base-metal mineralization is characterized by low Ca content as compared with that of QS alteration related to porphyry mineralization.

The chemical composition of dolomite from tourmaline–quartz–carbonate–muscovite alteration of the Peschanka deposit and NOF is similar to that from beresite (carbonate–muscovite–quartz–pyrite alteration) at intrusion-related gold deposits (Baksheev and Spiridonov, 1998; Generalov, 1990). In the both cases, dolomite is characterized by a low content of the kutnahorite end member (Fig. 6a).

The compositional evolution of carbonates in QSR II from calcite through dolomite to siderite results from the increasing activity of $CO_2$ in fluid (calcite to dolomite) (Martynov, 1991) followed by the decreasing activity of $H_2S$ (dolomite to siderite). According to Corbett and Leach (1998), the replacement of rhodochrosite by dolomite in argillic alteration indicates an increasing pH value of the mineral-forming solution. High Mn concentration in argillic carbonates of NOF is also typical of carbonates from quartz–illite alteration and related veins at postvolcanic epithermal Au–Ag deposits (Leroy et al., 2000; Spiridonov, 1992). Therefore, argillic alteration in NOF and related ore is regarded as epithermal, but is spatially related to the intrusive body.

## CONCLUSIONS

The data obtained indicate that two types of quartz–sericite alteration occur at porphyry copper deposits, which accompany porphyry and base-metal (subepithermal) ores. These types differ in: (1) chlorite in QSR I accompanying porphyry ore and carbonate in QSR II accompanying base-metal ore and (2) enrichment and depletion of dravite and oxy-dravite from QSR I and QSR II in Ca, respectively.

Argillic alteration differs from quartz–sericite alteration in the presence of illite and enrichment of chlorite in silica. In addition, rhodochrosite and Mn-rich dolomite develop in argillic alteration.

Illite from argillic alteration in porphyry systems is depleted in Al as compared with that from postvolcanic epithermal Au–Ag deposits.

## ACKNOWLEDGMENTS

We thank A.I. Brusnitsyn and S.F. Vinokurov, whose constructive comments have significantly

**Table 5.** Mineral assemblages of quartz–sericite and argillic alteration of the Peschanka deposit of Nakhodka ore field

| Type of altered rock | Mineralogy | Chemical composition of minerals | | | |
|---|---|---|---|---|---|
| | | chlorites | white micas | tourmaline | carbonates |
| Chlorite–quartz–muscovite (QSR I) | **chlorite, white micas, quartz,** *bornite*, *chalcopyrite* | Clinochlore (Si 2.80–3.12 apfu; $Fe_{tot}/(Fe_{tot} + Mg)$ 0.26–0.47), chamosite (2.72–3.05 apfu, 0.53–0.69); | Muscovite (2.80–3.03 apfu, 0.26–0.47), pahengite (3.29–3.30 apfu, 0.21–0.50) | | |
| Tourmaline–quartz–carbonate–muscovite ± phengite, QSR II | **white micas**, **tourmaline**, **carbonate**, **quartz**, *galena*, *sphalerite*, *fahlores*, *chalcopyrite* | | Muscovite (2.99–3.17 apfu, 0.27–0.47), phengite (3.26–3.30 apfu, 0.24–0.49) | Dravite, oxy-dravite (Ca up to 0.16 apfu) | Calcite, magnesite, dolomite (Mn up to 0.02 apfu) |
| Carbonate–quartz–illite | **white micas**, **carbonates**, **quartz**, *electrum*, *native gold*, *hessite*, Au–Ag *tellurides*, *arsenopyrite* | Clinochlore (Si 3.24–3.62 apfu) | Illite (3.08–3.43 apfu, 0.12–0.49) | | Rhodochrosite, calcite, dolomite (Mn up to 0.09–0.48 apfu) |

Rock-forming constituents are bolded.

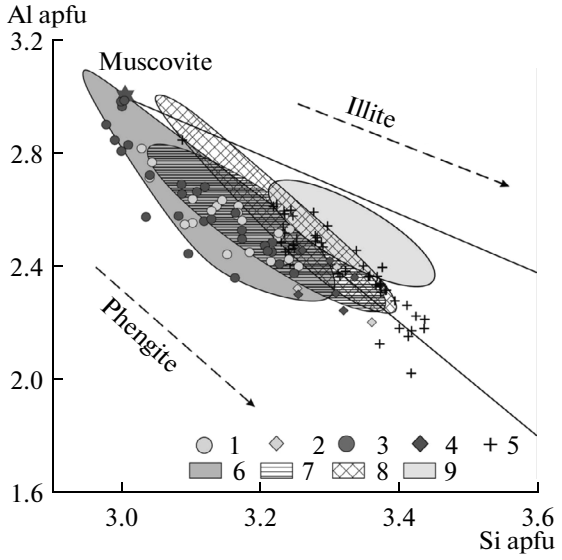


**Fig. 5.** An Al versus Si plot for white micas from altered rocks of various deposits modified after Carrillo-Rosúa et al. (2009). (1–4) Peschanka deposit and Nakhodka ore field: (1) muscovite of QSR I, (2) phengite of QSR I, (3) muscovite of QSR II, (4) phengite of QSR II; (5) illite of argillic rock; (6) muscovite of quartz–sericite rocks of Cu-Mo-porphyry deposits Yerington and Butte, US, Valley, Canada (Dilles et al., 2012), Erdenet, Mongolia, Zhireken, Aksug, and Sora, Russia (Sotnikov et al., 2002), Olkhovka, Russia (Rogacheva and Baksheev 2010); (7) muscovite from beresite of the Bestuybe, North Kazakhstan (Baksheev, 1996) and Berezovskii, Middle Urals (Baksheev and Kudryavtceva,1999) intrusion-related gold deposits; (8) illite from argillic rock of Yerington and Butte porphyry copper deposits, US (Dilles et al., 2012); (9) illite from quartz–sericite rock of the Palai-Islica Cu–Au volcanogenic deposit, Spain (Carrillo-Rosúa et al., 2009).

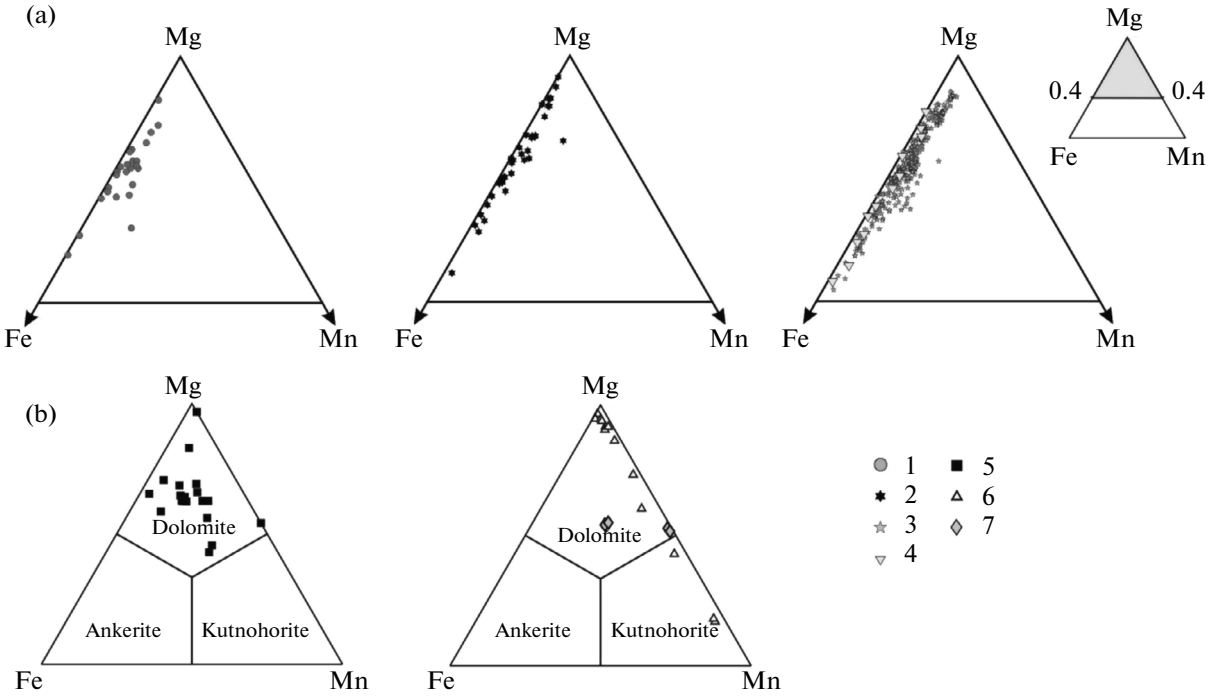


**Fig. 6.** Triangular diagrams in terms of Fe–Mg–Mn for dolomite group minerals. (a) Tourmaline–quartz–carbonate–muscovite ± phengite alteration of the Peschanka deposit and Nakhodka ore field, and beresite of intrusion-related gold deposits; (b) argillic rock of the Nakhodka ore field and volcanogenic gold deposits. (1) QSR II of the Peschanka deposit; (2) QSR II of the Nakhodka ore field; (3, 4) beresite of intrusion-related gold deposits: (3) Bestyube deposit, North Kazakhstan (Baksheev and Spiridonov, 1998), (4) deposit in Central Asia (Generalov, 1990); (5) argillic rock of the Nakhodka ore field; (6, 7) volcanogenic gold deposits: (6) Zod, Armenia (Spiridonov, 1992), (7) Cavnic, Romania (Leroy et al., 2000).

improved this paper. This study was supported by the Presidium of Russian Academy of Sciences (program "Basic Research for Development of Arctic Zone of the Russian Federation"), Russian Foundation for Basic Research (project no. 14-05-31198a) and Baimka Mining Company LLC.

## REFERENCES

Alva-Jimenez, T., Tosdal, R.M., Dipple, G., and Halley, S., Variation in hydrothermal muscovite composition around the Valley porphyry Cu–Mo deposit, Highland Valley district, British Columbia, Canada, *Proc. 11th SGA Biennial Meeting*, Antofagasta: Univ. Catolica Norte, 2011, pp. 340–342.

Bailey, S.W., Summary of recommendations of AIPEA nomenclature committee, *Clay Miner.*, 1980, vol. 15, pp. 85–93.

Baksheev, I.A., Mineralogy, zoning, and formation conditions of plutonogenic gold–antimony deposits hosted in black shale: a case study of the Bestyube deposit, Northern Kazakhstan, *Extended Abstract of Cand. Sci. (Geolmin) Dissertation*, Moscow: Moscow State University, 1996.

Baksheev, I.A. and Spiridonov, E.M., Carbonates of beresite and listvenite of the Bestyube deposit, *Vest. Mosk. Univ., Ser.4: Geol.*, 1998, no. 6, pp. 29–35.

Baksheev, I.A. and Kudryavtseva, O.E., Carbonates and white micas of beresite–listvenite as zoning indicators of the Berezovsky plutonogenic gold deposit, Midle Urals, in Ural'skaya letnyaya mineralogicheskaya shkola-99: Mater. nauch. shkoly (Ural Summer Mineral. School-99, Proc. Sci. School), Yekaterinburg, 1999, pp. 294–300.

Baksheev, I.A., Nikolaev, Yu.N., Prokof'ev, V.Yu., et al., Porphyry–epithermal gold–molybdenum–copper system of the Baimka trend, Western Cukchi Peninsula, in *Metallogeniya drevnikh i sovremennykh okeanov 2014: Mater. 20-i nauch. mol. shkoly* (Metallogeny of Ancient and Recent Oceans 2104: Proc. 20th Sci. School), Miass: Institute of Mineralogy, Ural Branch, Russian Academy of Sciences, 2014, pp. 108–112.

Carrillo-Rosúa, J., Morales-Ruano, S., Esteban-Arispe, I., and Hach-Alí, P.F., Significance of phyllosilicate mineralogy and mineral chemistry in an epithermal environment. insights from the Palai-Islica Au-Cu deposit (Almería, SE Spain), *Clays Clay Miner.*, 2009, vol. 57, no. 1, pp. 1–24.

Chitalin, A.F., Usenko, V.V., and Fomichev, E.V., The Baimka ore zone – a cluster of large base and precious metal deposits in the western Chukotka AD, *Mineral Res. Ross. Econ. Uprav.*, 2013, no. 6, pp. 68–73.

Corbett, G. and Leach, T.M., Southwest Pacific rim gold-copper systems: structure, alteration and mineralization, *Soc. Econ. Geol*, 1998, Spec. publ., vol. 6.

Dilles, J.H., Footprints of porphyry Cu deposits: Vectors to the hydrothermal center using mineral mapping and lithogeochemistry. http://minerals.usgs.gov/mrerp/reports/Dilles-G10AP00052.pdf. Cited July 6, 2014.

Le Fort, D., Hanley, J., and Guillong, M., Subepithermal Au–Pd mineralization associated with an alkalic porphyry Cu–Au deposit, Mount Milligan, Quesnel terrane, British Columbia, Canada, *Econ. Geol.*, 2011, vol. 106, pp. 781–808.

Generalov, M.E., Carbonates of gold deposit and formation conditions of carbonate-bearing mineral assemblages, *Vestn. Mosk. Univ., Ser. 4: Geol.*, 1990, no. 2, pp. 88–94.

Henry, D.J., Novák, M., Hawthorne, F., et al., Nomenclature of the tourmaline-supergroup minerals, *Am. Mineral.*, 2011, vol. 96, pp. 895–913.

Kaminskii, V.G., Comprehensive geological and prospecting model of porphyry copper deposit in the Baimka zone, *Sov. Geol.*, 1989, no. 11, pp. 46–56.

Kotova, M.S., Nagornaya, E.V., Anosova, M.O., et al., Dating of metasomatic process and ore-bearing granitoids of porhphyry copper prospects in the Nakhodka ore field, Wsetrn Chukchi Peninsula, in: Mater. V Ros. konf. po izotop. Geokhron (Proc. V Russ. Conf. Isotopic Geochron.), Moscow: Institute of Geochemistry and Analytical Chemistry, Rusisan Academy of Sciences, 2012, pp. 181–184.

Leroy, J.L., Hube, D., and Marcoux, E., Episodic deposition of Mn minerals in cockade breccia structures in three low-sulfidation epithermal deposits: a mineral stratigraphy and fluid-inclusion approach, *Can. Mineral.*, 2000, vol. 38, pp. 1125–1136.

Martínez-Serrano, R.G. and Dubois, M., Chemical variations in chlorite at the los humeros geothermal system, mexico, *Clays Clay Miner.*, 1998, vol. 46, pp. 615–628.

Martynov, K.V., Equlibria of rocks-forming carbonates under hydrothermal conditions, *Extended Abstract of Cand. Sci. (Geolmin) Dissertation,* Moscow: MSU, 1991.

Migachev, I.F., Shishakov, V.B., Sapozhnikov, V.G., and Kaminskii, V.G., Ore and alteration zoning of porphyry copper deposit in the Northeastern Russia, *Geol. Rudn. Mestorozhd.*, 1984, vol. 26, no. 5, pp. 91–94.

Migachev, I.F. and Girfanov, M.M., Shishakov, V. B. The Peschanka porphyry copper deposit, *Rudy Met.*, 1995, no. 3, pp. 48–58.

Nikolaev, Yu.N, Baksheev, I.A., Prokof'ev, V.Yu., et al., Precious metal mineralization of the Baimka trend, Western Chukchi Peninsula: mineralogy, geochemistry, and fluid inclusions, *Geol. Ore Deposits*, (in press).

Rogacheva, L.I. and Baksheev, I.A., Mineralogy of metasomatic rocks and geochronology of the Olhovka porphyry copper deposit, Chukotka, Russia, *33rd Ann. General Meet. MDSG*, Glasgow: Univ. Glasgow, 2010, pp. 39–40.

Shapovalov, B.C., Some geochemical features of ores in the Baimka cluster, in *Rudnye formatsii Severo-Vostoka SSSR* (Ore Types of Northeastern USSR), Magadan: SVKNII DVO Akad. Nauk SSSR, 1990, pp. 162–170.

Sillitoe, R.H., Porphyry copper systems, *Econ. Geol.*, 2010, vol. 105, pp. 3–41.

Sotnikov, V.I., Berzina, A.T., and Berzina, A.P., Fluorine in white micas of Siberian and Mongolian porphyry copper–molybdenum deposits and its probable origin, *Geochem. Int.*, 2002, vol. 40, no. 10, pp. 1106–1114.

Spiridonov, E.M., Listvenite and zodite, *Geol. Rudn. Mestorozhd.*, 1991, vol. 33, no. 2, pp. 38–48.

Volchkov, A.G., Sokirkin, G.I., and Shishakov, V.F., Geology and ores of the Anyui porphyry copper deposits, northeastern USSR *Geol. Rudn. Mestorozhd.*, 1982, no. 4, pp. 89–94.

Zharikov, V.A., Rusinov, V.L., Marakushev, A.A., et al., *Metasomatizm i metasomaticheskie porody* (Metasomatism and Metasomatic Rocks), Moscow: Nauchnyi mir, 1998.

*Translated by I. Baksheev*